ISLAMIC UNIVERSITY OF TECHNOLOGY, (IUT)

Intelligent Optimized Design of PI Current Controller of LCL Filter Using PSO in Grid Connected Converters

By

Mohammad Ashif Iqbal (092464)

Muhammad Rubaiyet Islam Ratul (092460)

Shahkat Ahmed(092457)

A Dissertation

Submitted in Partial Fulfillment of the Requirement for the

Bachelor of Science in Electrical and Electronic Engineering

Academic Year: 2012-2013

Department of Electrical and Electronic Engineering.

Islamic University of Technology (IUT)

A Subsidiary Organ of OIC.

Dhaka, Bangladesh.

A Dissertation on,

Intelligent Optimized Design of PI Current Controller of LCL Filter Using PSO in Grid Connected Converters.

Submitted By

Mohammad Ashif Iqbal (092464) Muhammad Rubaiyet Islam Ratul Shahkat Ahmed(092457)

Approved By

Dr. Md. Shahid Ullah

Professor & Head of the

Department of EEE, IUT.

Dr.Kazi Khairul Islam

Thesis Supervisor

Professor

Department of EEE, IUT

Abstract

The use of Dispersed or Distributed Resources (DR) is rapidly increasing in modern distribution networks because of their potential advantages. As many types of these resources generate electrical energy in the form of dc voltage source, they need a dc/ac converter for energy transfer to the grid through a simple L filter to reduce the injected current harmonics. However, LCL filters can provide better harmonic attenuation and reduce the filter size at the same time. This paper is concerned with the subject of grid connected converters using LCL filter topology. Basic expressions related to LCL filters are derived and compared to that of L filter. The control strategy is briefly described and it is shown that how the system can be stabilized by proper state plus output.

Now LCL filters have become more and more popular and the design of LCL filter has become a hot research topic in industry field. The requirement when design a LCL filter is to achieve the required filter effort with inductor and capacitor value as small as possible. In 2005, Marco Liserre presented a step by step design method to design the filter which is an effective method in article for the first time.

Recently, artificial intelligence has become a popular search technique used in computing to find exact or approximate solutions to optimization and search problems. There are many kinds of artificial intelligence and Genetic Algorithm (GA) is used mostly. Genetic algorithms are a particular class of evolutionary algorithms that use techniques inspired by evolutionary biology such as inheritance, mutation, selection, and crossover. It become successful because of it's concise arithmetic describing. But recently, the Particle Swam Optimization (PSO) is proved to an effective optimal arithmetic which is a novel kind of global Optimization. Compared to GA, PSO don't have to operate crossover and mutation so it is easier and faster to optimize.

Preface

The undergraduate thesis, "Intelligent Optimized Design of PI Current Controller of LCL Filter Using PSO in Grid Connected Converters" has been written for the completion of Bachelor of Science degree at Islamic University of Technology, Bangladesh. This thesis work and writing has been done during the year 2013 under the supervision of Dr. Kazi Khairul Islam, Professor of the department of Electrical and Electronic Engineering.

We would like to dedicate this thesis to Mr. Ashik Ahmed along with our superviser. Without the dedicated help of him we won't be able to complete this work. We are also grateful to all of our will-wishers, who provided their perpetual support towards accomplishing this task successfully.

Contents

1. Introduction.
2. Background and Theory
   - 2.1 Three Phase Systems
     - 2.1.1 Symmetrical Components - The positive-, negative- and zero-sequence
     - 2.1.2 αβ-transformation
     - 2.1.3 dq-transformation
   - 2.2 The Voltage Source Converter (VSC)
     - 2.2.1 Switching in the VSC
   - 2.3 LCL Filter
     - 2.3.1 Mathematical Model
     - 2.3.2 State-space model of the LCL circuit
     - 2.3.3 State space model of the VSC
3. Controller
   - 3.1 Proportional Control
   - 3.2 Integral Control
   - 3.3 Derivative Control
   - 3.4 Control Requirements
   - 3.5 Proportional Integral Control
     - 3.5.1 Tuning of the PI Controller for the Current Loop
     - 3.5.2 State-space model of the current controller
   - 3.6 State Space Model including the PI Current Controller

4. System Design

4.1 LCL-filter parameters

4.2 PI Current Controller Parameters

5. Particle Swarm Optimization

5.1 Background

5.2 Optimization

5.3 Pseudo Code

5.4 Flow Chart

Conclusion

List of Figures

2.1 The Grid Thevenin Equivalent
2.2 Symmetrical Components
2.3 Positive and negative sequence in an unbalanced system
2.4 Voltage and current vector in αβ-coordinates
2.5 Voltage and current vector in dq-coordinates
2.6 Two level - three phase voltage source converter
2.9 Block diagram of VSC

3.1 PI current controller with decoupling between the d-axis and theq-axis
3.2 Current Loop for the PI controller

List of Parameters

Parameter	*Explanation*
d	Real axis of the Park Transformation
q	Imaginary axis of the Park Transformation
abc	Phases of a three-phase system
pu	pu value
g	Value at the grid
$conv$	Value at the converter
b	Base value
α	Real axis of the Clark transformation
β	Imgainary axis of the Clark transformation
LL	Line to line value
up	Upper value of the band limit
low	Lower value of the band limit
RMS	Root mean square value
ref	Reference value
$+$	Positive Sequence components
$-$	Negative Sequence components
0	Zero Sequence components

L_g	Grid Inductance
R_g	Grid side Resistance
C_f	Filter capacitance

ω_b	Base angular frequency
τ_i	Regulator Parameter
T_a	VSC time constant

K_p	Regulator Parameter
K_i	Regulator Parameter

Chapter 1
Introduction

Nowadays, there is a common understanding that the global warming is human made, with the energy sector as the main contributor to the green house gas emissions. In Europe, the energy sector alone contributes with 80% of the green house gas emissions. The demand for energy worldwide is at the same time continuously increasing. This has led to a significant attention towards alternative energy resources, and the amount of renewable energy integrated into the power system has grown rapidly during the last years. Due to the stochastic behavior of the input power from many of the new renewable energy sources and the large intervention of the renewable systems, the implementation of them will have an impact on the operation of the power system. Hence, more stringent grid connection is required. The use of power electronic equipment has then become an essential part for the utilization of the renewable energy generation systems. Especially the Voltage Source Converter (VSC) topology is becoming a standardmodular solution due to its capability for reversible flow, DC-voltage control and the implementation of high performance control system . Although many different control structures have been developed for VSC's in various application, the VSC for grid connection is often current controlled. The current controller as the inner control loop of a cascaded control system appears to be the most commonly used control structure . With current control as the inner control loop, the overall operation will depend on the performance of the current controllers. This has led to significant attention in literature towards development and evaluation of different control structures for the VSC. The control system should be designed for stable operation under every grid condition, but weak grid conditions, caused by a high value of the grid impedance is one issue that can challenge the control of the VSC. There has so far been given little attention towards control and operation of a VSC in connection with a weak grid, while taking into account the dynamics of the inner current control loop and the interaction between the converter and the grid impedance. Remote faults in distribute power systems results in voltage dips through the power system . In areas with high share of decentralized distributed gen-eration, there is grid code requirements for generator "ride-through" where the generator is imposed to stay connected during transient faults. Both balanced and unbalanced changes in the voltage may occur, and affect the operation of the converter in different ways. Hence the current control of the VSC should be able to handle operation under both balanced and unbalanced conditions.

The motivation of this thesis is therefore to investigate, compare and evaluate different current control strategies when a VSC is connected to a weak point in the power system under various grid conditions. The following current control strategies will be presented in investigated: 1) The Decoupled Proportional Integrator (PI) controller in the synchronous rotating reference frame. Recently, artificial intelligence has become a popular search technique used in computing to find exact or approximate solutions to optimization and search problems. There are many kinds of artificial intelligence and Genetic Algorithm (GA) is used mostly. Genetic algorithms are a particular class of evolutionary algorithms that use techniques inspired by evolutionary biology such as inheritance, mutation, selection, and crossover. It become successful because of it's concise arithmetic describing. But recently, the Particle Swam Optimization (PSO) is proved to an effective optimal arithmetic which is a novel kind of global Optimization. Compared to GA, PSO don't have to operate crossover and mutation so it is easier and faster to optimize. This paper present a new design method using genetic algorithm and particle swam optimization which combined the advantages of the above the design methods.

Chapter 2

Background and Theory

2.1 Three Phase Systems

A symmetrical three phase voltage source can be represented by three voltage vectors with the same length and the phase shifted with 120◦ with respect to each other, as described in Equation 2.1. The three phases are named abc in this thesis.

$$\begin{bmatrix} V_a \\ V_b \\ V_c \end{bmatrix} = \begin{bmatrix} V\cos(\omega t) \\ V\cos(\omega t - \frac{2\pi}{3}) \\ V\cos(\omega t + \frac{2\pi}{3}) \end{bmatrix} \tag{2.1}$$

If the symmetrical system is connected with a common isolated neutral the currents and the voltage for the three phase system fulfills the conditions of Equation 2.2.

$$i_a + i_b + i_c = 0 \tag{2.2}$$

$$v_a + v_b + v_c = 0$$

The Thevenin equivalent

A power system can be large and complex with several nodes that connects a number of lines with transformers and generators or loads. During calculation of the performance of one particular node without doing a full scale analysis of the entire network, the network can be represented with its thevenin equivalent This thevenin equivalent is shown in Figure 2.1 and the calculation of Z can be found by the fault level Sk

at the node by Equation 2.3 .

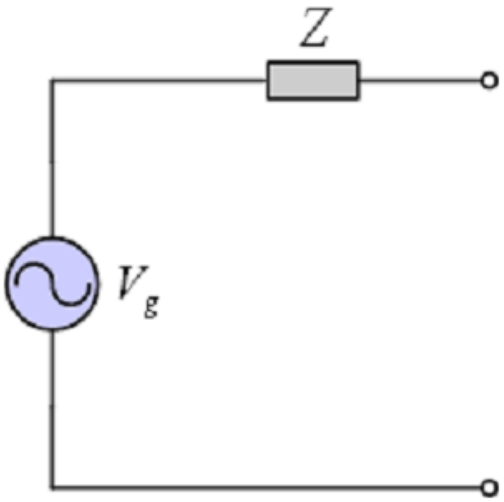

Figure 2.1: The grid Thevenin equivalent

$$|Z| = \frac{V^2}{S_k} \tag{2.3}$$

Where Sk is calculated from short circuit analysis of the power system and V is the nominal line-to-line voltage at the node. The thevenin equivalent voltage Vg can be taken as the nominal voltage at the point of interest. The fault level can now be expressed by the X/R ratio in Z = R + jX . The fault level is an important parameter, not only during fault conditions, but it is also predicting the performances during normal operation, as it defines the strength of the of the network at the particular point. A weak grid is a network or a part of a network where the fault level is low, that is if Z is high, and indicates that the node voltage is fragile with respect to changes in active and reactive power flow at the node.

2.1.1 Symmetrical Components - The positive-, negative-and zero-sequence

Ideally, the voltages and the currents will be perfectly balanced and symmet-rical, which leads to greatly simplified analysis. However, this is not always the case. To analyze the three phase system under unbalanced conditions, thesystem can be decomposed by use of symmetrical components which mathemat-ically breaks an unbalanced systems into three balanced sequences. A positive-, negative- and zero-sequence. The theory of symmetrical components comes from a paper written by Fortescue in 1918 [6]. The paper demonstrate that N set of unbalanced phasors could be expressed as the sum of N symmetrical sets of balanced phasors. The unsymmetrical voltage and currents are found by super-position of the three sequences. The voltage can be written as in Equation 2.4 and the phasors of the three phases in the positive- negative- and zero-sequence, with superscript respectively +, − and 0, are shown in Figure 2.2a-2.2c.

$$\begin{bmatrix} V_a \\ V_b \\ V_c \end{bmatrix} = \begin{bmatrix} V_a^- \\ V_b^- \\ V_c^- \end{bmatrix} + \begin{bmatrix} V_a^- \\ V_b^- \\ V_c^- \end{bmatrix} + \begin{bmatrix} V_a^0 \\ V_b^0 \\ V_c^0 \end{bmatrix} \tag{2.4}$$

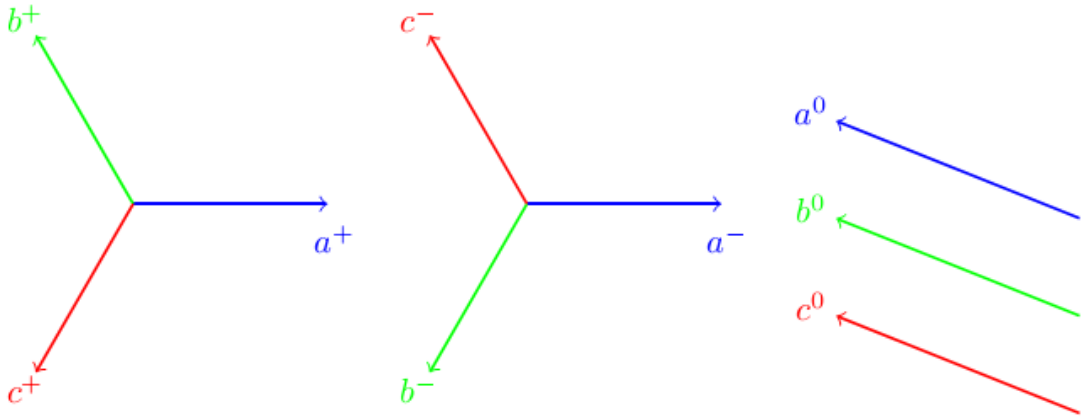

(a) Positive sequence (b) Negative Sequence (c) Zero sequence

Figure 2.2: Symmetrical components

The steady state vector representation in Figure 2.2a-2.2c, has been derived in and can be written as in Equation 2.5 and becomes as in Equation 2.6 in the time domain . A zero sequence current may be present when there is a path in addition to the three lines, f.ex earth .

$$\begin{bmatrix} V_a \\ V_b \\ V_c \end{bmatrix} = \begin{bmatrix} 1 & 1 & 1 \\ 1 & h & h^2 \\ 1 & h^2 & h \end{bmatrix} \begin{bmatrix} V_a^+ \\ V_a^- \\ V_a^0 \end{bmatrix} \tag{2.5}$$

2.1.2 αβ-transformation

The three phases, both voltage and current, can be represented in a two phase representation. The momentarily value of the three phases can be transformedinto a voltage vector or a current vector. This vector can then be represented in a orthogonal stationary αβ-reference as shown in Figure 2.4. The transformation from the abc reference to the αβ-reference is shown in Equation 2.7.

$$\begin{bmatrix} X_\alpha \\ X_\beta \\ X_\gamma \end{bmatrix} = \frac{2}{3} \begin{bmatrix} \cos(0) & \cos(\frac{2\pi}{3}) & \cos(-\frac{2\pi}{3}) \\ \sin(0) & \sin(\frac{2\pi}{3}) & \sin(-\frac{2\pi}{3}) \\ \frac{1}{2} & \frac{1}{2} & \frac{1}{2} \end{bmatrix} \begin{bmatrix} X_a \\ X_b \\ X_c \end{bmatrix}$$

Introducing the positive- and the negative- sequence and ignoring the zero sequence component, the voltage transformed into in the αβ-reference frame is given by Equation

$$\begin{bmatrix} V_\alpha \\ V_\beta \end{bmatrix} = V^+ \begin{bmatrix} \cos(\omega t) \\ \sin(\omega t) \end{bmatrix} + V^- \begin{bmatrix} \cos(-\omega t + \phi^-) \\ \sin(-\omega t + \phi^-) \end{bmatrix}$$

The positive sequence voltage is supposed as the phase origin. The voltage vector consists of two sub vectors. One rotating in the positive direction and one rotating in the negative direction. Nor the magnitude or the rotational frequency of the voltage vector for an unbalanced system is constant .

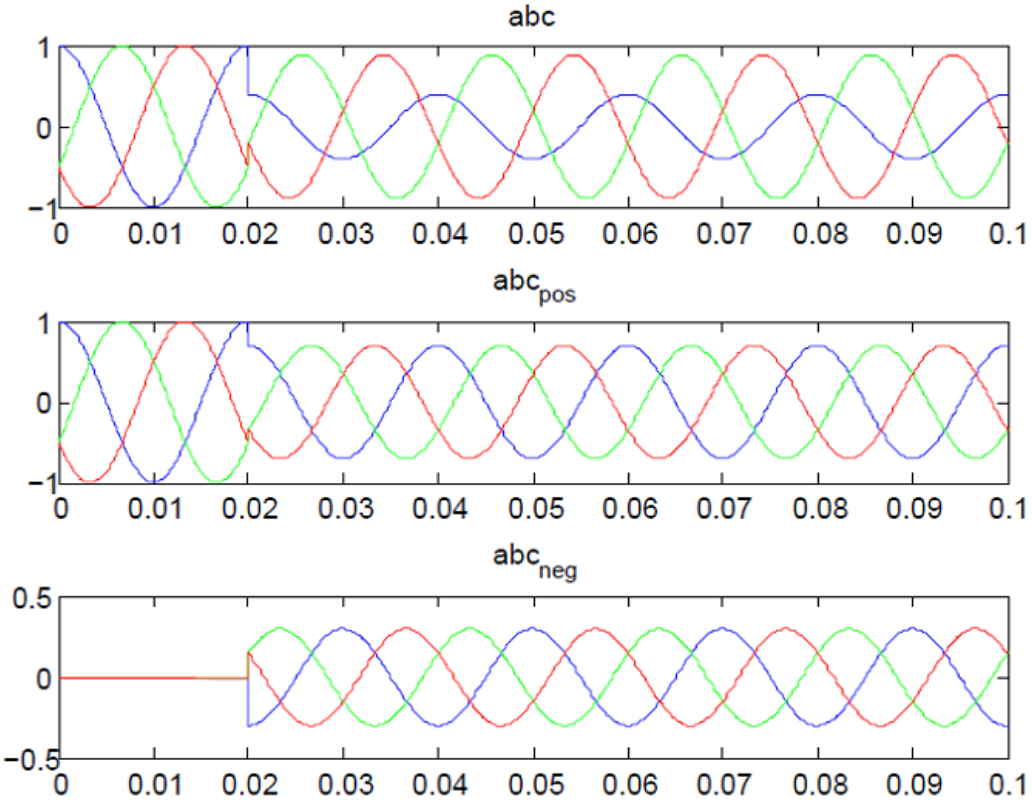

Figure 2.3: Positive and negative sequence in an unbalanced system

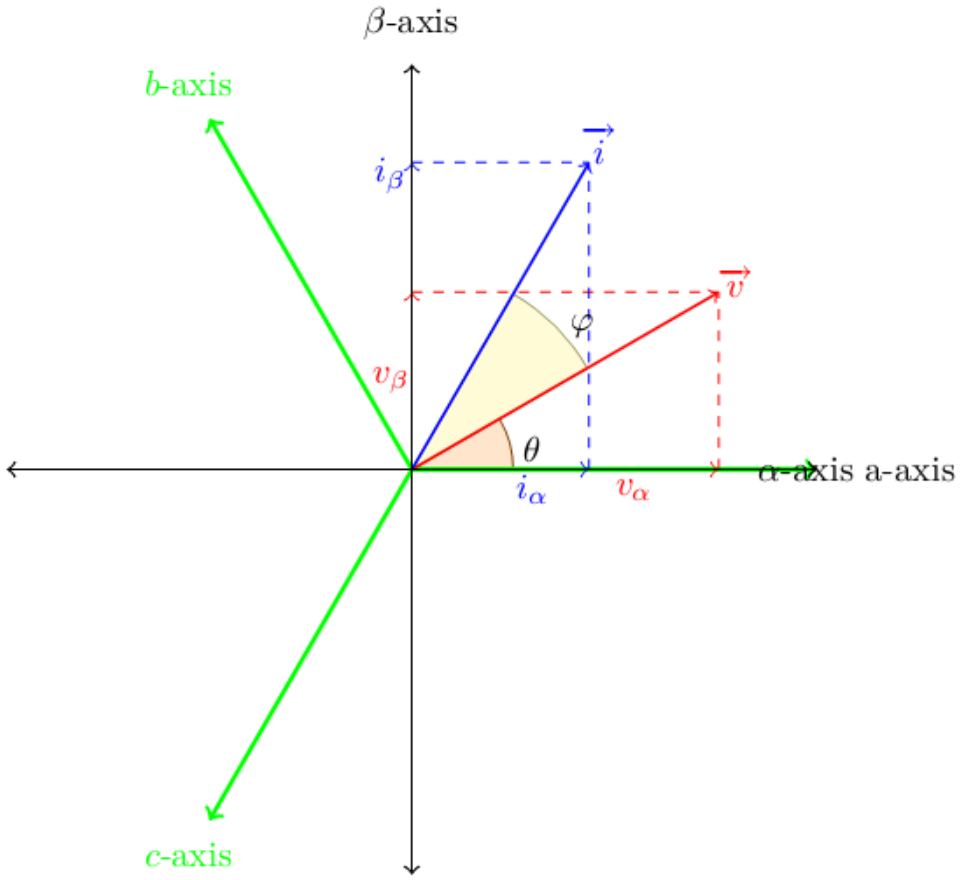

Figure 2.4: Voltage and current vector in $\alpha\beta$-coordinates.

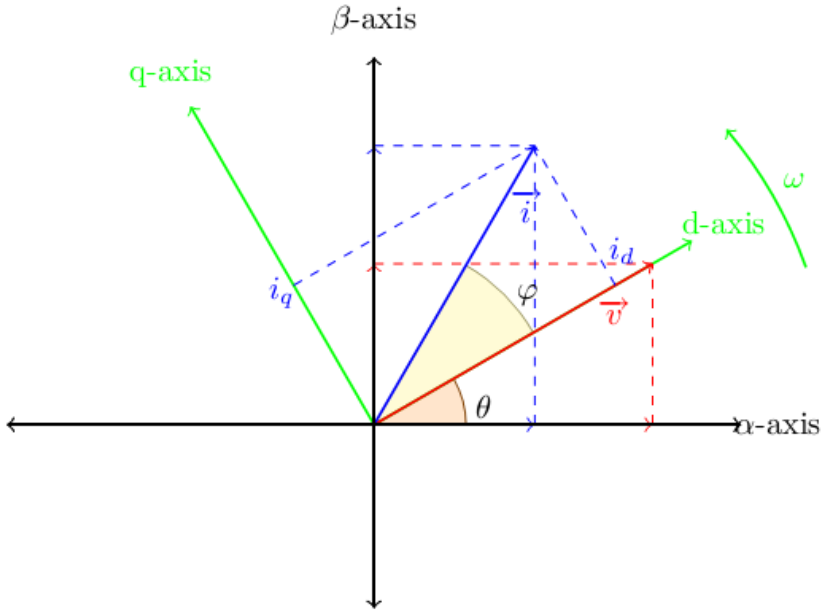

Figure 2.5: Voltage and current vector in dq-coordinates.

2.1.3 dq-transformation

The voltage and current vectors can be represented in any coordinate system. The synchronous rotating reference (SRF)-dq coordinate system is rotating in the same angular speed as the voltage vector. Since the voltage vector and the coordinate system are aligned, the electrical components in this system behaves like DC components. This gives some obvious benefits in control manners. The transformation from αβ-reference to dq-reference is shown in Equation 2.9 and in Figure 2.5 :

$$\begin{bmatrix} X_d \\ X_q \end{bmatrix} = \begin{bmatrix} \cos(\theta) & \sin(\theta) \\ -\sin(\theta) & \cos(\theta) \end{bmatrix} \begin{bmatrix} X_\alpha \\ X_\beta \end{bmatrix}$$

Since the voltage vector for the park transformation is aligned with the d-axis, the q component of the voltage vector is zero. The active and reactive power is then reduced to the control of id and iq as shown in Equation 2.10.

$$p = \frac{3}{2} v_d i_d$$

$$q = -\frac{3}{2} v_d i_q$$

2.2 The Voltage Source Converter (VSC)

There are different ways of converting and inverting voltage with power elec-tronic devices. For distributed generation the state of the art is the two level three phase converter. For high power wind turbines a three-level neutral point clamped VSC is an option. Also matrix converters and multilevel converters

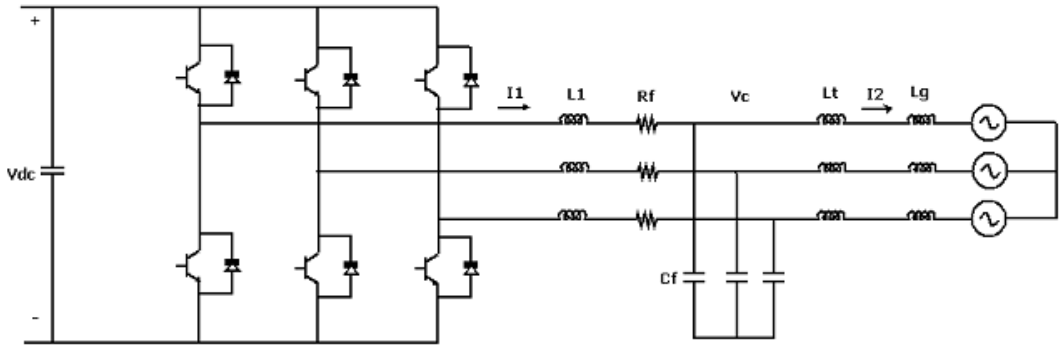

Figure 2.6: Two level - three phase voltage source converter

are developing and been implemented in distribution power generation systems. This thesis will focus on the control of a three-phase two level VSC.

2.2.1 Switching in the VSC

By use of different combinations of the switches in the converter the voltage vec-tor can be represented by eight space vectors. Since the three phases are shifted 120 degrees with respect to each other, combination of the the six switches on the three legs and phases will give the the following voltage vector representa-tions:

$$\overrightarrow{v_k} = \begin{cases} (\frac{2}{3})V_{DC}e^{j\pi(k-1)/3} & \text{for} \quad k = 1, ...6 \\ 0 & \text{for} \quad k = 0, 7 \end{cases}$$

This give six nonzero voltage vectors and two zero voltage vectors. Figure2.8 shows the

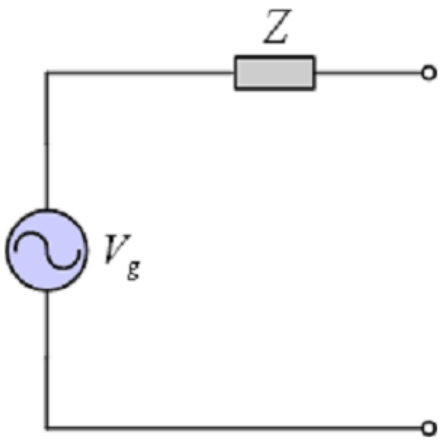

Figure 2.1: The grid Thevenin equivalent

$$\Delta i_{L1,max} = \frac{V_{DC}}{8L_1 f_{SW}}$$

The selection of current ripple is a trade off between the size of L1 , switching losses and inductor coil and core losses [40]. The choice of the capacitor is done based on the evaluation of the reactive power in the capacitor and in the inductance. The resonance frequency of the system, ignoring the resistance for simplifi-cations, is given by Equation 2.20.

$$f_{res} = \frac{1}{2\pi}\sqrt{\frac{L_1 + L_2 + L_g}{L_1(L_2 + L_g)C_f}}$$

The LCL filter itself is independent of the power level and the switching frequency as seen in Equation 2.20,but the LCL-filter resonance should be lower for lower switching frequencies to achieve better filtering. The switching in the VSC should be lower for higher power levels .

If the grid voltage is balanced the ripple in the current, for the use of a L-filter is described in and given by Equation 2.22.

$$i_{ripple}(t) = \frac{1}{L}\int_0^t v_{ripple}(\tau)d\tau$$

2.3.1 Mathematical Model

When designing the control structure for the current, it is useful to have a model of the converter to design the controller properly. In , a mathematical model for a three phase voltage source converter, is presented. The system is assumed balanced. This model includes the effect of the switches, and the switching function. The dq representation in a synchronous reference frame is shown in Equation 2.23

$$u_{DC} = (\frac{3}{2}(i_q d_q + i_d d_d) - i_{DC})\frac{1}{sC}$$
$$i_d = (u_{DC}d_d - v_d + \omega L i_q)\frac{1}{R+sL}$$
$$i_q = (u_{DC}d_q - v_q - \omega L i_d)\frac{1}{R+sL}$$

This model can be simplified by merging the DC-voltage v dc and the switch-ing function d to an average v conv . The VSC will then have a vector representa-tion as shown in Equation 2.24, the current is defined positive in direction from the VSC towards the grid as shown in Figure 2.6.

$$\frac{d}{dt}\begin{bmatrix} i_d \\ i_q \end{bmatrix} = \begin{bmatrix} -\frac{R}{L} & \omega \\ -\omega & -\frac{R}{L} \end{bmatrix}\begin{bmatrix} i_d \\ i_q \end{bmatrix} + \begin{bmatrix} v_{d,conv} - v_d \\ v_{q,conv} - v_q \end{bmatrix}$$

$$\frac{d}{dt}\begin{bmatrix} i_{d,pu} \\ i_{q,pu} \end{bmatrix} = \begin{bmatrix} -\frac{\omega_b R_{pu}}{L_{pu}} & \omega \\ -\omega & -\frac{\omega_b R_{pu}}{L_{pu}} \end{bmatrix}\begin{bmatrix} i_{d,pu} \\ i_{q,pu} \end{bmatrix} + \frac{\omega_b}{L}\begin{bmatrix} v_{d,conv,pu} - v_{d,pu} \\ v_{q,conv,pu} - v_{q,pu} \end{bmatrix}$$

This gives the block diagram of the VSC as shown in the Figure 2.9 The switching in the PWM can be mathematical modeled as a time delay for control manners. The 1.order transfer function approximation for the time delay is as in Equation 2.26 .

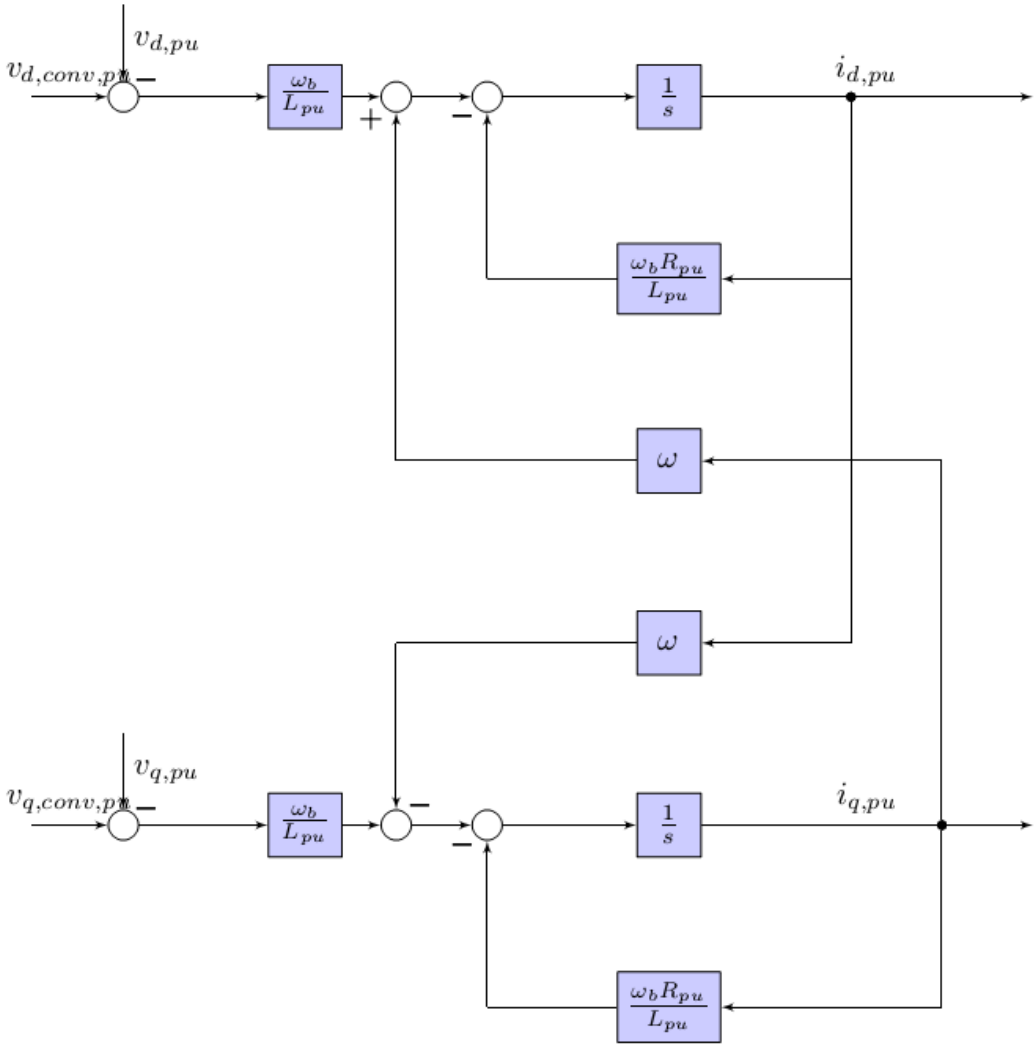

Figure 2.9: Block diagram of VSC

2.3.2 State-space model of the LCL circuit

The state space model presented in this thesis is largely based on the work done in , and modified to describe the system under investigation. The LC-circuit is described in Equation 2.23 and shown with pu-values in Figure 2.9. To include the capacitor in the filter and the weak grid thevenin equivalent inductance, that influences the point of synchronization, Equation 2.27 and Equation 2.28 are added to the mathematical model.

$$i_{od} = (v_{cd} - v_{od} + \omega L_g i_{oq}) \frac{1}{R_g + sL_g}$$
$$i_{oq} = (v_{cq} - v_{oq} - \omega L_g i_{od}) \frac{1}{R_g + sL_g}$$

$$v_{cd} = (i_d - i_{od} + \omega C v_{cq}) \frac{1}{sC}$$
$$v_{cq} = (i_q - i_{oq} - \omega C v_{cd}) \frac{1}{sC}$$

Where Lg and Rg are the grid side inductance and resistance in the weak grid thevenin equivalent. The state vector, the input vector and the output vector for this LCL-circuit subsystem is shown in Equation 2.29, Equation 2.30 and Equation 2.31 respectively.

$$\mathbf{x_{LCL}} = [i_{d,pu}\ i_{q,pu}\ i_{0,pu}\ v_{cd,pu}\ v_{cq,pu}\ v_{c0,pu}\ i_{od,pu}\ i_{oq,pu}\ i_{o0,pu}]^T$$

$$\mathbf{u_{LCL}} = [v_{d,conv,pu}\ v_{q,conv,pu}\ v_{0,conv,pu}\ v_{od,pu}\ v_{oq,pu}\ v_{o0,pu}\ \omega]^T$$

$$\mathbf{y_{LCL}} = [i_{d,pu}\ i_{q,pu}\ i_{0,pu}\ v_{cd,pu}\ v_{cq,pu}\ v_{c0,pu}\ i_{od,pu}\ i_{oq,pu}\ i_{o0,pu}]^T$$

$$\dot{\mathbf{x}}_{\mathbf{LCL}} = \mathbf{A_{LCL}}\mathbf{x_{LCL}} + \mathbf{B_{LCL}}\mathbf{u_{LCL}} + \mathbf{R_{LCL}}(\mathbf{x_{LCL}}, \mathbf{u_{LCL}})$$

Where:

$$\mathbf{A_{LCL}} = \begin{bmatrix}
-\frac{\omega_b R_{pu}}{L_{pu}} & 0 & 0 & -\frac{\omega_b}{L_{pu}} & 0 & 0 & 0 & 0 & 0 \\
0 & -\frac{\omega_b R_{pu}}{L_{pu}} & 0 & 0 & -\frac{\omega_b}{L_{pu}} & -\frac{\omega_b}{L_{pu}} & 0 & 0 & 0 \\
0 & 0 & -\frac{\omega_b R_{pu}}{L_{pu}} & 0 & 0 & 0 & -\frac{\omega_b}{C_{pu}} & 0 & 0 \\
\frac{\omega_b}{C_{pu}} & 0 & 0 & 0 & 0 & 0 & 0 & -\frac{\omega_b}{C_{pu}} & 0 \\
0 & \frac{\omega_b}{C_{pu}} & 0 & 0 & 0 & 0 & 0 & 0 & -\frac{\omega_b}{C_{pu}} \\
0 & 0 & \frac{\omega_b}{C_{pu}} & 0 & 0 & 0 & -\frac{\omega_b R_{g,pu}}{L_{g,pu}} & 0 & 0 \\
0 & 0 & 0 & \frac{\omega_b}{L_{g,pu}} & 0 & 0 & 0 & -\frac{\omega_b R_{g,pu}}{L_{g,pu}} & 0 \\
0 & 0 & 0 & 0 & \frac{\omega_b}{L_{g,pu}} & 0 & 0 & 0 & -\frac{\omega_b R_{g,pu}}{L_{g,pu}} \\
0 & 0 & 0 & 0 & 0 & & & &
\end{bmatrix}$$

$$\mathbf{B_{LCL}} = \begin{bmatrix} \frac{\omega_b}{L_{pu}} & 0 & 0 & 0 & 0 & 0 & 0 \\ 0 & \frac{\omega_b}{L_{pu}} & 0 & 0 & 0 & 0 & 0 \\ 0 & 0 & \frac{\omega_b}{L_{pu}} & 0 & 0 & 0 & 0 \\ 0 & 0 & 0 & 0 & 0 & 0 & 0 \\ 0 & 0 & 0 & 0 & 0 & 0 & 0 \\ 0 & 0 & 0 & 0 & 0 & 0 & 0 \\ 0 & 0 & 0 & \frac{\omega_b}{L_{g,pu}} & 0 & 0 & 0 \\ 0 & 0 & 0 & 0 & \frac{\omega_b}{L_{g,pu}} & 0 & 0 \\ 0 & 0 & 0 & 0 & 0 & \frac{\omega_b}{L_{g,pu}} & 0 \end{bmatrix}$$

$$\mathbf{R_{LCL}} = \begin{bmatrix} \omega i_{q,pu} \\ -\omega i_{d,pu} \\ 0 \\ \omega v_{cq,pu} \\ -\omega v_{cd,pu} \\ 0 \\ \omega i_{oq,pu} \\ -\omega i_{0d,pu} \\ 0 \end{bmatrix}$$

2.3.3 State space model of the VSC

The state space model is a simplification of the system, and do not include the switches and the physical consequences of the voltage on the converter side of the filter being turned on and off. In the state space representation of the system, the converter is represented as a 1.order time delay approximation as in Equation 2.26. The state space model of the converter then becomes as in Equation 2.37

$$\mathbf{x_{VSC}} = \frac{d}{dt} \begin{bmatrix} v^*_{d,conv,pu} \\ v^*_{q,conv,pu} \end{bmatrix} = \begin{bmatrix} -\frac{1}{T_a} & 0 \\ 0 & -\frac{1}{T_a} \end{bmatrix} \begin{bmatrix} v^*_{d,conv,pu} \\ v^*_{q,conv,pu} \end{bmatrix} + \frac{1}{T_a} \begin{bmatrix} v_{d,conv,pu} \\ v_{q,conv,pu} \end{bmatrix}$$

Chapter 3

Controller

3.1 Proportional Control

Open Loop Control

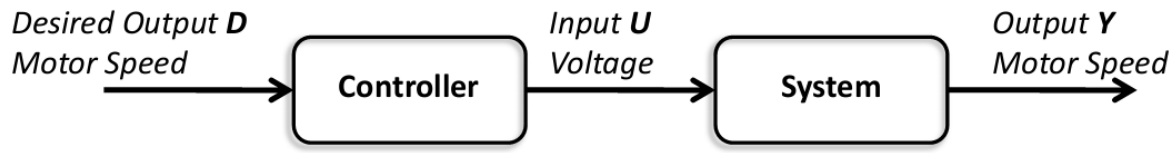

User determines desired response
Controller is an electronic amplifier, determines input voltage
Amplifier voltage U = K . D where K is a Gain
Actual motor speed depends on motor dynamics and load disturbances

Closed Loop Control

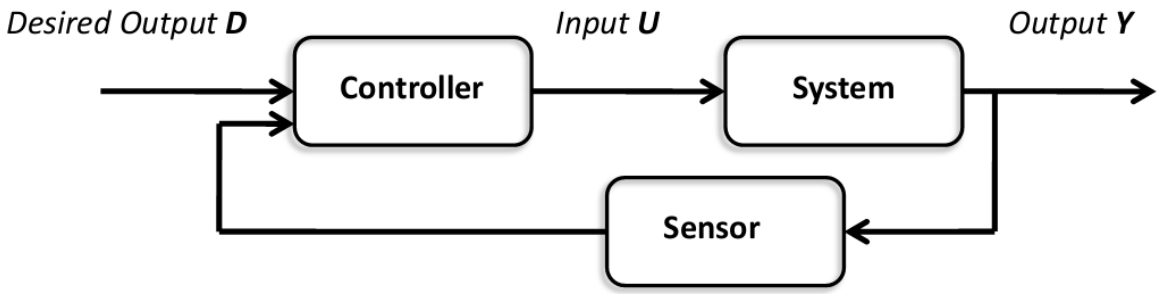

Output is measured with a suitable sensor
Controller compares desired output with actual output
An electronic amplifier produces a voltage
proportional to the error U = K . (D – Y)
Reduces Sensitivity to disturbance

Closed Loop Transfer Function

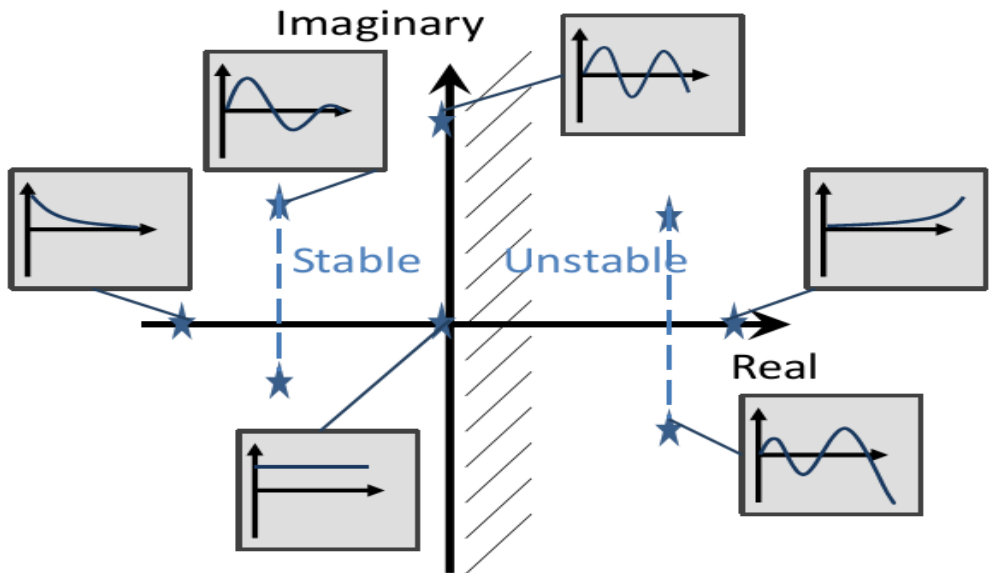

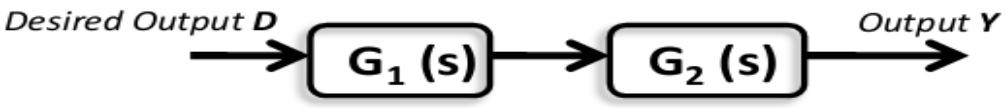

$$Y = G_1(s)\, G_1(s)\, D$$

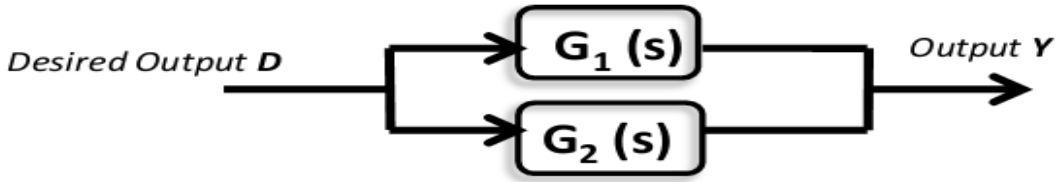

$$Y = G_1(s) + G_1(s)\, D$$

$$Y = \frac{G_1(s)}{1 + G_1(s)G_2(s)} \times D$$

3.2 Integral Control

- Gain is applied to integral of error Proportional to both magnitude & duration
- Summing error over time gives an accumulated offset previously uncorrected
- Results in Zero Steady State Error
- Can cause overshoot of set point
- Greater complexity in closed loop Transfer Function – may become unstable

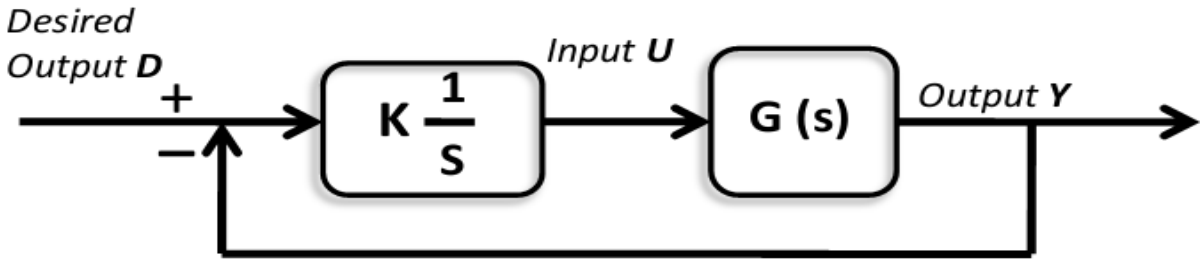

Closed Loop Transfer Function

Y =

Y =

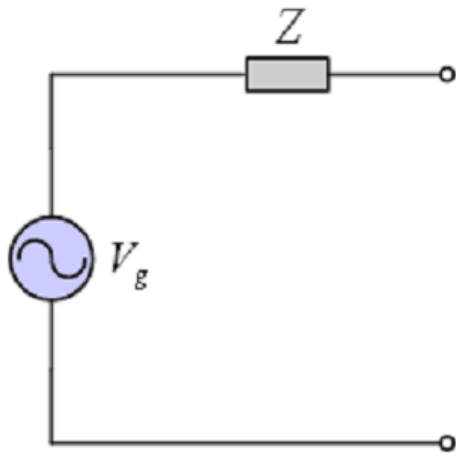

Figure 2.1: The grid Thevenin equivalent

3.3 Derivative Control

- Gain is applied to rate of change of error
- Acts to slowdown change
- Most noticeable near set point

- Used to reduce magnitude of overshoot
- Used in combination with Proportional and/or Integral gains
- Greater complexity in closed loop Transfer Function – may become unstable due to Sensitivity to noise

3.4 Control Requirements

Control Gains Summary

Proportional Gain

Applicable to Error between setpoint & output
Larger values → faster response
Very large values → process instability and oscillation.
Results in Steady State Error

Integral Gain

Proportional to integral of Error between setpoint & output
Larger values → steady state errors rapidly eliminated.
Overshoot may lead to instability
Zero Steady State Error

Derivative Gain

Proportional to derivative of Error between setpoint & output
Larger values → decreased overshoot, but slower transient response
May lead to instability due to signal noise amplification in the differentiation of the error

3.5 Proportional Integral Control

Used; where systems are predominantly 1 ST
Order
Ensures; Zero Steady State Error (if closed loop transfer function is stable)
Increased set point tracking speed
However; Increased complexity introduces a Phase Lag ; reducing stability

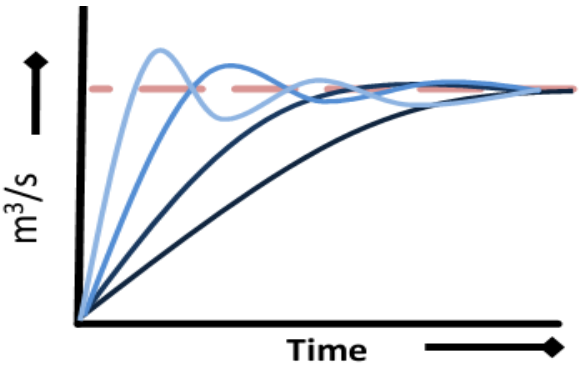

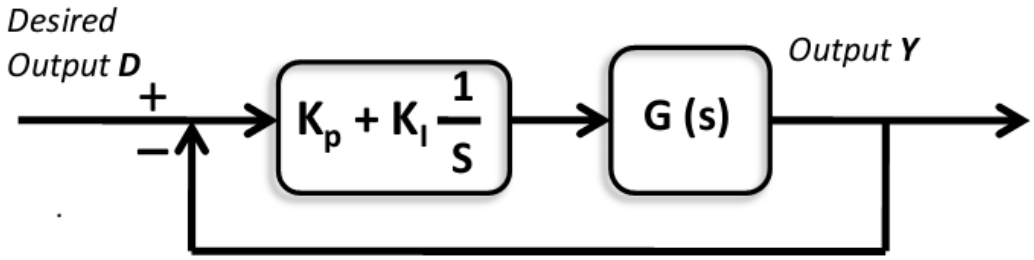

Closed Loop Transfer Function

$$Y = \frac{G(s K_p + K_I)}{s + G(s K_p + K_I)} \times D$$

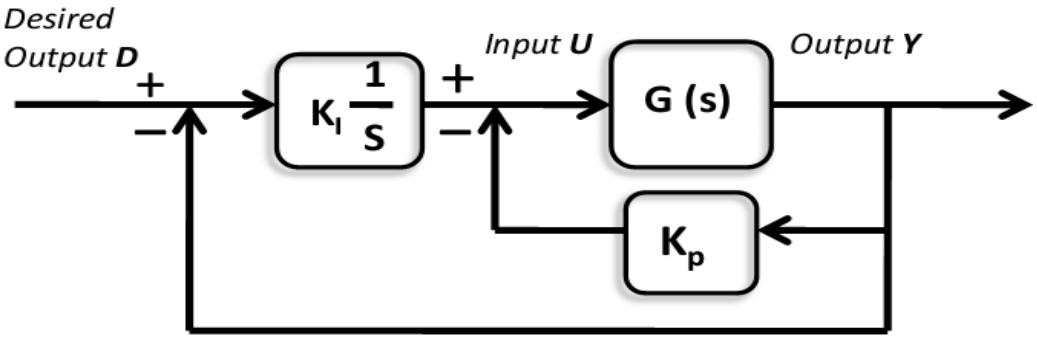

3.5.1 Tuning of the PI Controller for the Current Loop

$$K_{p,pu} = \frac{\tau_{pu} R_{pu}}{2T_a}$$

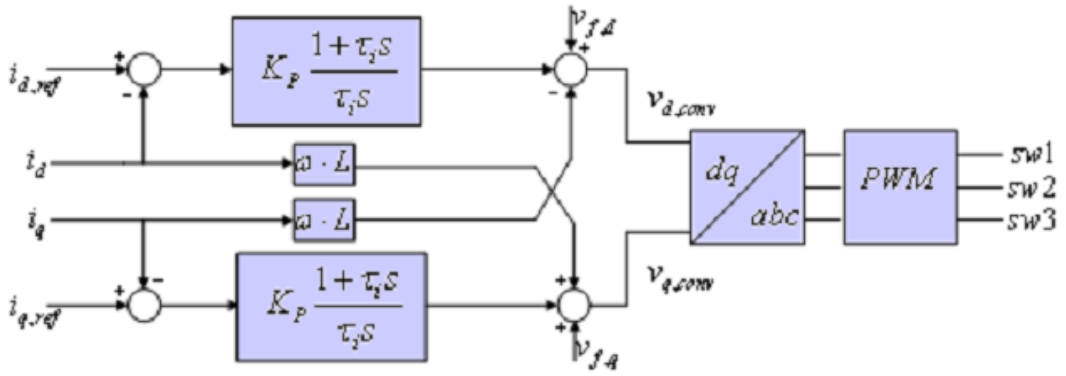

3.1 : PI current controller with decoupling between the d-axis and theq-axis

and

$$\tau_i = \tau_{pu}$$

Where

$$\tau_{pu} = \frac{L_{pu}}{\omega_b R_{pu}}$$

$$H_{OL} = \frac{K_{p,pu}}{\tau_{pu} R_{pu}} \frac{1}{s(1+T_a s)}$$

$$H_{CL}(s) = \frac{\frac{K_{p,pu}}{R_{pu}\tau_i T_a}}{s^2 + \frac{1}{Ta}s + \frac{K_{p,pu}}{R_{pu}\tau_i T_a}}$$

The bandwidth of the system is defined, by the Nyquist criteria, as the frequency where the gain of the open loop transfer function crosses -3dB line or the phase delay becomes greater than 45 degrees. Since this do not always occur at the same time, the definition that gives the smallest bandwidth should be chosen . The damping factor and the undamped natural frequency is given by equa-tion 2.67 and 2.68 .

$$\omega_n = \sqrt{\frac{K_{p,pu}}{\tau_{pu} R_{pu} T_a}} = \frac{1}{\sqrt{2} T_a}$$

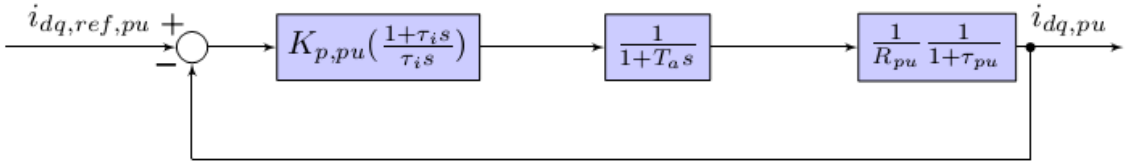

FIG : Current Loop for the PI controller

$$\xi = \frac{1}{2}\sqrt{\frac{\tau_{pu} R_{pu}}{K_{p,pu} T_a}} = \frac{1}{\sqrt{2}}$$

3.5.2 State-space model of the current controller

These state variables can be obtained as a charge, since its the integral of the current. The state vector is given in 2.69, the input vector is given in 2.71 and the output vector as in 2.70.

$$\mathbf{x_{cc}} = [q_{ld}^{err} \; q_{lq}^{err}]^T$$

$$\mathbf{y_{cc}} = [v_{d,conv,pu} \; v_{q,conv,pu}]^T$$

$$\mathbf{u_{cc}} = [i_{d,ref,pu} \; i_{q,ref,pu} \; i_{d,pu} \; i_{q,pu} \; v_{cd,pu} \; v_{cq,pu} \; \omega]^T$$

The state space model of the current controller has a standard linear form, but the A-matrix is zero because of the new variables which do not include internal feedback.

$$\dot{\mathbf{x}}_{\mathbf{cc}} = \mathbf{A_{cc}} \mathbf{x_{cc}} + \mathbf{B_{cc}} \mathbf{u_{cc}}$$

$$\dot{\mathbf{x}}_{\mathbf{cc}} = \begin{bmatrix} 0 & 0 \\ 0 & 0 \end{bmatrix} \begin{bmatrix} q_{ld}^{err} \\ q_{lq}^{err} \end{bmatrix} + \begin{bmatrix} 1 & 0 & -1 & 0 & 0 & 0 & 0 \\ 0 & 1 & 0 & -1 & 0 & 0 & 0 \end{bmatrix} \begin{bmatrix} i_{d,ref} \\ i_{q,ref} \\ i_d \\ i_q \\ v_{cd} \\ v_{cq} \\ \omega \end{bmatrix} \quad (2.72)$$

$$\mathbf{y}_{\mathbf{cc}} = (\mathbf{C}\mathbf{x}_{\mathbf{cc}} + \mathbf{D}\mathbf{u} + \mathbf{S}(\mathbf{u}))$$

$$\mathbf{y}_{\mathbf{cc}} = \begin{bmatrix} K_i & 0 \\ 0 & K_i \end{bmatrix} \begin{bmatrix} q_{ld}^{err} \\ q_{lq}^{err} \end{bmatrix}$$

$$+ \begin{bmatrix} K_{p,pu} & 0 & -K_{p,pu} & 0 & 1 & 0 & 0 & 1 & 0 \\ 0 & K_{p,pu} & 0 & -K_{p,pu} & 0 & 1 & 0 & 0 & 1 \end{bmatrix} \begin{bmatrix} i_{d,ref} \\ i_{q,ref} \\ i_d \\ i_q \\ v_{cd} \\ v_{cq} \\ \omega \\ i_{ad,d} \\ i_{ad,q} \end{bmatrix} + \begin{bmatrix} -\omega i_{q,pu} \\ \omega i_{d,pu} \end{bmatrix} \quad (2.73)$$

3.6 State Space Model including the PI Current Controller

The VSC is a complex dynamic system that interacts with the grid. The model of the integration of VSC in DG systems must include all the dynamics of the converter in the frequency range of interest. This model should then include both the LCL filter in the interface between the converter and the grid, and the control system associated with the converter circuit. A single state-space model which includes the physical model and the transformation, current control and the PLL is derived in and modified in this thesis. The state-space model will be in the form given by Equation 2.75.

Complete State-space Model

$$x_{tot} = \begin{bmatrix} q_{ld}^{err} & q_{lq}^{err} & v_{d,conv}^{*} & v_{q,conv}^{*} & v_{d,conv} & v_{q,conv} & i_d & i_q & v_{cd} & v_{cq} & i_{gd} & i_{gq} & i_{od} & i_{oq} \end{bmatrix}$$

$$A_{tot} = \begin{bmatrix} A_{CC} & 0 & 0 \\ 0 & A_{VSC} & 0 \\ 0 & 0 & A_{LCL} \end{bmatrix}$$

$$A_{Total} = \begin{bmatrix} -\frac{k_i}{k_p} & 0 & 0 & 0 & \frac{1}{k_p} & 0 & -\frac{w}{k_p} & 0 & 0 & 0 & 0 & 0 \\ 0 & -\frac{k_i}{k_p} & 0 & 0 & 0 & \frac{1}{k_p} & 0 & -\frac{w}{k_p} & 0 & 0 & 0 & 0 \\ 0 & 0 & -\frac{1}{T_a} & 0 & \frac{1}{T_a} & 0 & 0 & 0 & 0 & 0 & 0 & 0 \\ 0 & 0 & 0 & -\frac{1}{T_a} & 0 & \frac{1}{T_a} & 0 & 0 & 0 & 0 & 0 & 0 \\ 0 & 0 & 0 & 0 & 0 & 0 & 0 & 0 & 0 & 0 & 0 & 0 \\ 0 & 0 & 0 & 0 & 0 & 0 & 0 & 0 & 0 & 0 & 0 & 0 \\ 0 & 0 & \frac{w_b}{L} & 0 & 0 & 0 & -\frac{R_{wb}}{L} & w & -\frac{w_b}{L} & -\frac{w_b}{L} & 0 & 0 \\ 0 & 0 & 0 & \frac{w_b}{L} & 0 & 0 & -w & -\frac{R_{wb}}{L} & 0 & 0 & 0 & 0 \\ 0 & 0 & 0 & 0 & 0 & 0 & \frac{w_b}{C} & 0 & 0 & 0 & -\frac{w_b}{C} & 0 \\ 0 & 0 & 0 & 0 & 0 & 0 & 0 & 0 & \frac{w_b}{L_g} & \frac{w_b}{L_g} & -\frac{R_{gwb}}{L} & w \\ 0 & 0 & 0 & 0 & 0 & 0 & 0 & 0 & 0 & 0 & -w & -\frac{R_{gwb}}{L} \\ 0 & 0 & 0 & 0 & 0 & 0 & 0 & \frac{w_b}{C} & -w & -w & 0 & -\frac{w_b}{C} \end{bmatrix}$$

Chapter 4

System Design

4.1 LCL-filter parameters

Parameter	PU-Value
L	0.05
Lg	0.05
R	0.00109
Rg	0.00109
C	0.1
w	314.16
wb	576

Eigen Values

-6.28+11834j
-6.28-11834j
-6.28+11206j
-6.28-11206j
-13+314j
-13-314j

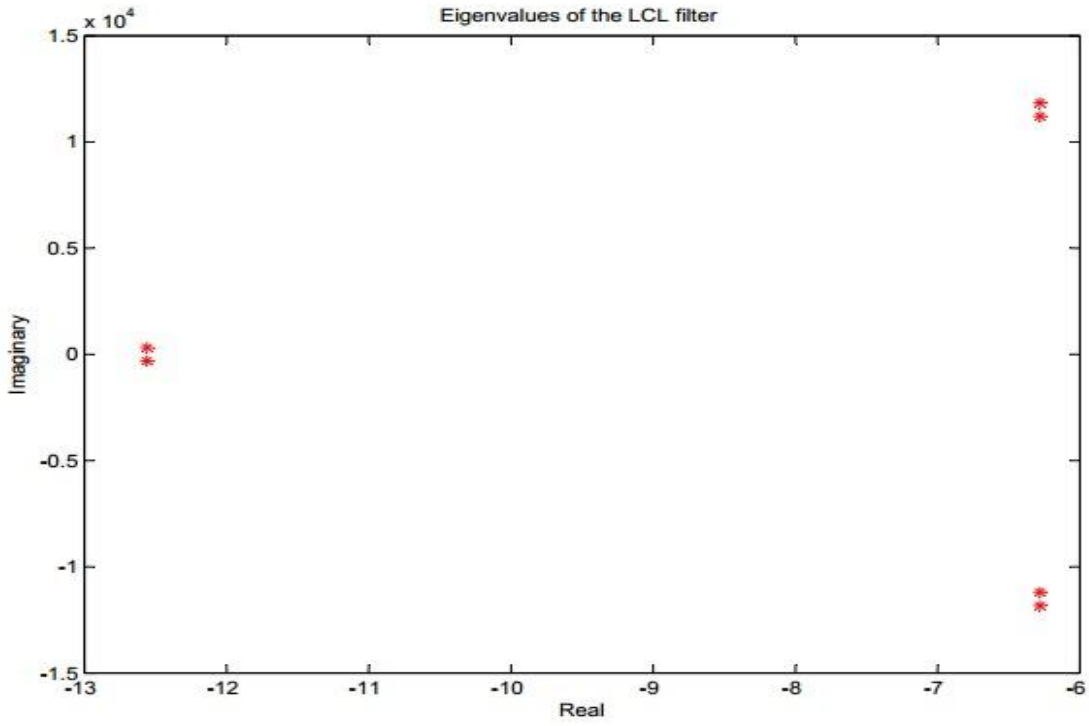

4.2 PI Current Controller Parameters

Parameter	Value
R	0.00109
Rg	0.00109
L	1.1 micro H
Lg	10 micro H
C	0.1
Kp	0.4757
Ki	3.37
Ta	0.00143
Wb	576 Hz
Wn	314.16rad/sec

Eigen Values:

0
0
-6+11742i
-6-11742i
-6+11298i
-6-11298i
-13+9i
-13-9i
-699
-699
0
0

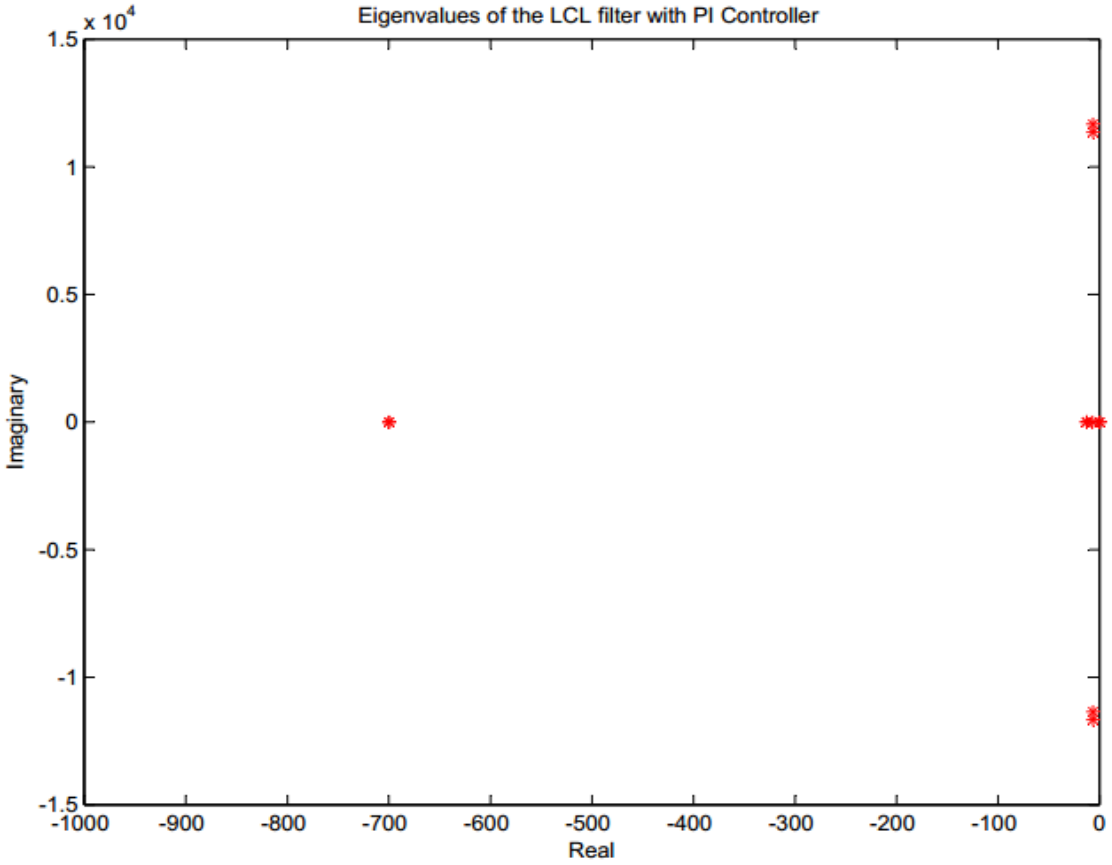

Chapter 5

Particle Swarm Optimization

5.1 Background

Particle Swarm Optimization (PSO) is a technique used to explore the search space of a given problem to find the settings or parameters required to maximize a particular objective. This technique, first described by James Kennedy and Russell C. Eberhart in 1995 , originates from two separate concepts: the idea of swarm intelligence based off the observation of swarming habits by certain kinds of animals (such as birds and fish); and the field of evolutionary computation. This short tutorial first discusses optimization in general terms, then describes the basics of the particle swarm optimization algorithm.

5.2 Optimization

Optimization is the mechanism by which one finds the maximum or minimum value of a function or process. This mechanism is used in fields such as physics, chemistry, economics, and engineering where the goal is to maximize efficiency, production, or some other measure. Optimization can refer to either minimiza-tion or maximization; maximization of a function f is equivalent to minimization of the opposite of this function, −f [4]. Mathematically, a minimization task is defined as:

Given $f : R^n \rightarrow R$
Find $\hat{x} \in R^n$ such that $f(\hat{x}) \leq f(x), \forall x \in R^n$

Similarly, a maximization task is defined as

Given $f : R^n \rightarrow R$
Find $\hat{x} \in R^n$ such that $f(\hat{x}) \geq f(x), \forall x \in R^n$
The domain R^n of f is referred to as the search space (or parameter space [2]). Each element of R^n is called a candidate solution in the search space, with $\hat{x}$ being the optimal solution. The value n denotes the number of dimensions of the search space, and thus the number of parameters involved in the optimization problem. The function f is called the objective function , which maps the search space to the function space. Since a function has only one output, this function space is usually one-dimensional. The function space is then mapped to the one-dimensional fitness space, providing a single fitness value for each set of parameters. This single fitness value determines the optimality of the set of parameters for the desired task. In most cases, including all the cases discussed in this paper, the function space can be directly mapped to the
itness space. However, the distinction between function space and fitness space is important in cases such as multi objective optimization tasks, which include several objective functions drawing input from the same parameter space [2, 5]. For a known (differentiable) function f , calculus can fairly easily provide us with the minima and maxima of f . However, in real-life optimization tasks, this objective function f is often not directly known. Instead, the objective function is a "black box" to which we apply parameters (the candidate solution) and receive an output value. The result of this evaluation of a candidate solution becomes the solution's fitness. The final goal of an optimization task is to find the parameters in the search space that maximize or minimize this fitness. In some optimization tasks, called constrained optimization tasks, the elements in a candidate solution can be subject to certain constraints (such as being greater than or less than zero) . For the purposes of this paper, we will focus on unconstrained optimization tasks. A simple example of function optimization can be seen in Figure 1. This figure shows a selected region the function f , demonstrated as the curve seen in the diagram. This function maps from a one-dimensional parameter space—the set of real numbers R on the horizontal x-axis—to a one-dimensional function space— the set of real numbers R on the vertical y-axis. The x-axis represents the candidate solutions, and the y-axis represents the results of the objective function when applied to these candidate solutions. This type of diagram demonstrates what is called the fitness landscape of an optimization problem. The fitness landscape plots the n-dimensional parameter space against the one-dimensional fitness for each of these parameters.

Each particle tries to modify its position using following information:

>the current positions
>the current velocities
>distance between current positions and pbest
>distance between current positions and gbest

The modifications of particle's positions can be mathematically modeled by the following equations:

$$V_i^{k+1} = wV_i^k + c_1 rand_1(\dots) * \left(pbest_i - s_i^k\right) + c_2 rand_2(\dots) * \left(gbest - s_i^k\right)$$

Where V_i^k=velocity of agent i at iteration k
w=weighting function
c_j=weighting factor
s_i^k=current position of agent i at iteration k
$pbest_i$=pbest of agent i
gbest=gbest of the group

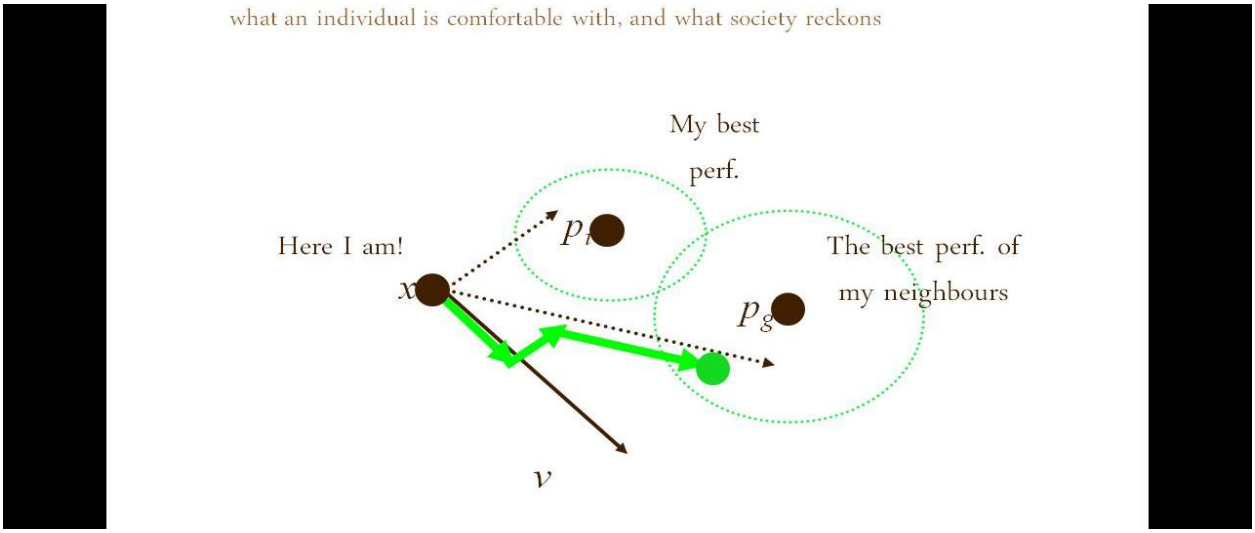

A particle have three tendencies-
1)Following its own way.
2)Going back more or less towards the best previous position.
3)Going more or less towards his best neighbor.

Now, according to PSO the particle will combine these tendencies in order to globally efficient.

5.3 Pseudo Code

```
For each particle
{
   Initialize particle
}
Do until maximum iterations or minimum error criteria
{
   For each particle
   {
      Calculate Data fitness value
      If the fitness value is better than pBest
      {
         Set pBest = current fitness value
      }
      If pBest is better than gBest
      {
         Set gBest = pBest
      }
   }

   For each particle
   {
      Calculate particle Velocity
      Use gBest and Velocity to update particle Data
   }
```

5.4 Flow Chart

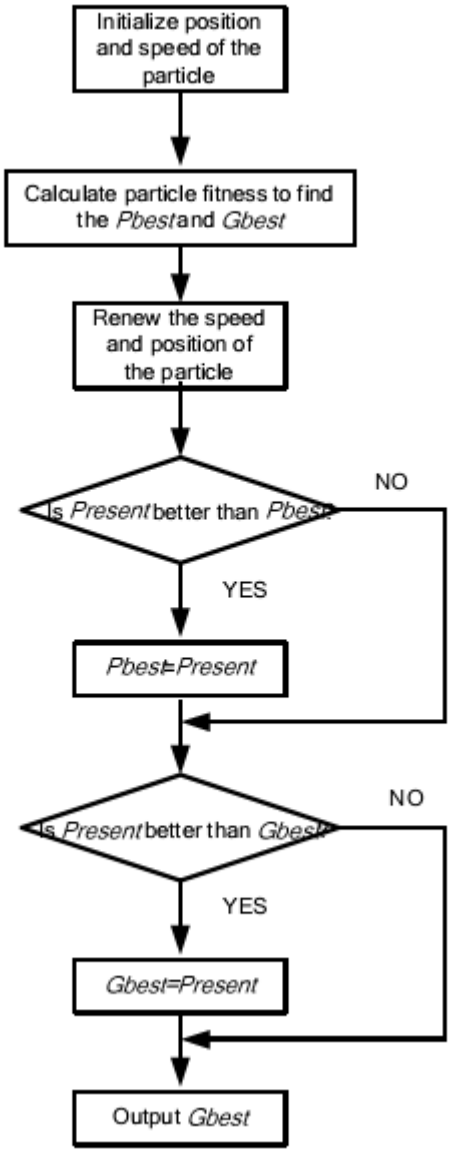

Final Tuned Value of k_p and k_i using PSO algorithm:

Kp =6.0996

Ki = 0.1628

Eigen Values

0
0
-6+11742i
-6-11742i
-6+11298i
-6-11298i
-13+9i
-13-9i
-699
-699
0
0

.

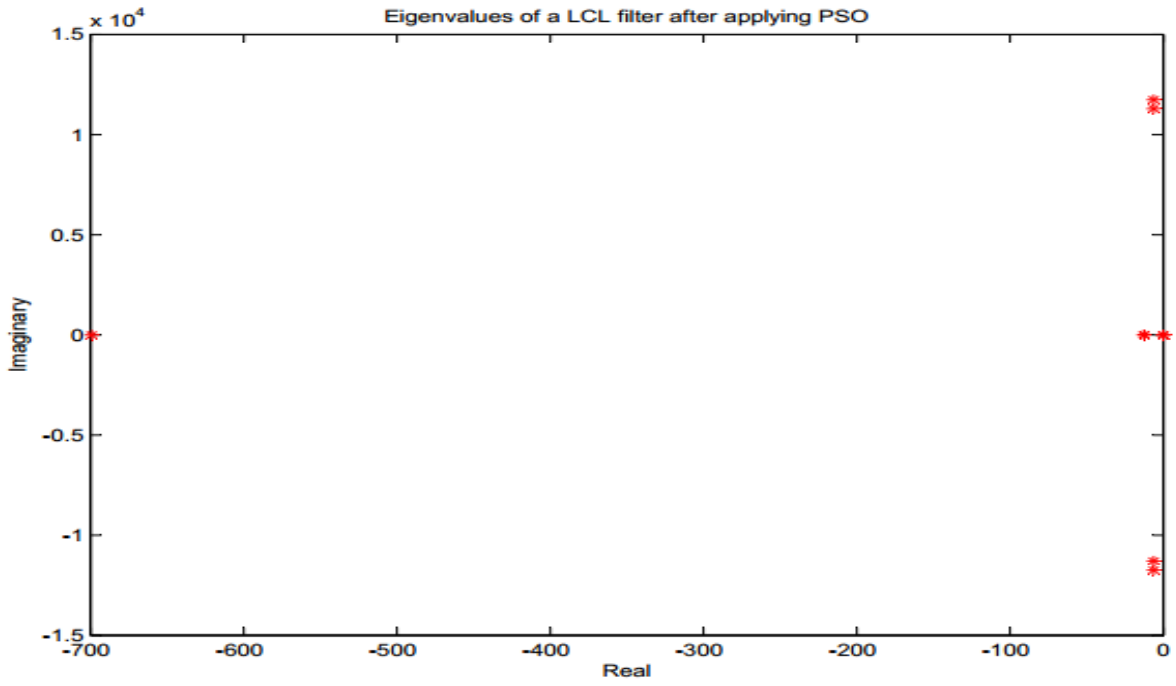

Conclusion

The work presented in this thesis is an initial study of the influence that a weak grid has on the response and stability of current controllers for a Voltage Source Converter. Different control structures have been evaluated by compar-ison based on different simulation cases. The operation of the converter for the simulated cases does not necessarily represent the preferred performance, but it show trends that indicate a general behavior during different type of converter-operation under various grid conditions. It is verified that a weak grid, represented by a large grid inductance, can make the system become unstable and controllers plays a significant role in provoking such instability mechanisms. This is particularly the case for the PI controller in the syn-chronous reference frame. Then write the design program by intelligent optimization algorithm.The simulation results indicate that PSO has a better convergence and more effective. In practical application, PSO is easy to realize and has less calculation work

References

[1] H.R Karshenas and H. Saghafi , Performance Investigation of LCL filters in Grid Connected Converters, 2006 IEEE PES Transmission and Distribution Conference and Exposition Latin America, Venezuela.

[2] M. Liserre, F. Blaabjerg, and S. Hansen “Design and Control of an LCLFilter-Based Three-Phase Active Rectifier,” IEEE Trans. Industry Applications, vol. 41, no. 5, pp. 1281-1291, September/October 2005

[3]M. Lindgren and J. Svensson,” Control of a Voltage-source Converter Connected to the Grid through an LCL-filter-Application to Active Filtering," in Proc. PESC'98, vol. 1, pp. 229-235.

[4] Tarjei Midtsund, Control of Power Electronic Converters in Distributed Power Generation Systems.

[5] Wei Sun, Zhe Chen and Xiaojie Wu “Intelligent Optimize Design of LCL Filter for Three Phase Voltage-Source PWM Rectifier”.

[6] M.Lindgren, J.Svensson. Connecting fast switching Vlotage-source converters to the Grid-Harmonic Distortion and its reduction. IEEE Strock Power Tech Conference, Stockholm, June 18-22, 1995, Proceedings of Power Electronics: 191-195.

[7] Marco Liserre, Frede Blaabjerg, Steffan Hansen. Design and Control of an LCL-filter based Three-phase Active Rectifier. IEEE Transactions on Industry Applications, September/October, 2005: 1281-1291.

[8] Xianping Zhang, Yaxi Li. Analysis and Design of LCL Type Filter for Three- phase Voltage Source Rectifier[J]. Electrotechnical Application. 2007,26(5) ： 65-68.

[9] F. Blaabjerg, R. Teodorescu, M. Liserre, A. V. Timbus, “Overview of Control and Grid Synchronization for Distributed Power Generation Systems,” IEEE Transactions on Industrial Electronics, Vol. 53, No. 5, Oct. 2006, pp. 1398-1409.

[10] M. P. Kaźmierkowski, M. A. Dzieniakowski, “Review of Current Regulation Methods For VS-PWM Inverters,” in Proc. of IEEE International Symposium on Industrial Electronics,ISIE’93, 1-3. June 1993, Budapest, Hungary, pp. 448-456